

Monitoring of bridge vibrations with image-assisted total stations

Matthias Ehrhart¹, Slaven Kalenjuk¹, and Werner Lienhart¹

¹ Institute of Engineering Geodesy and Measurement Systems (IGMS), Graz University of Technology, Graz, Austria

ABSTRACT: Vibration-based Structural Health Monitoring (SHM) has become increasingly popular during the last years. Hereby, the frequencies of the structure's oscillations form the basis of the structural diagnostics. The typically used measurement sensors for determining these frequencies include accelerometers and robotic total stations which comprise the drawback that access to the monitored structure is required. To overcome this limitation, the usage of an image-assisted total station (IATS) is proposed. Hereby, the measurement procedure is similar to measurements with conventional robotic total stations in which the retroreflective prism can be omitted for IATS measurements. Instead, prominent natural features of the monitored structure are observed by using the IATS's telescope camera and later analyzed by means of image processing techniques. Along with a saving of costs, access to the monitored structure is not required which allows a more flexible definition of the measurement points. To demonstrate the suitability of an IATS for vibration monitoring, experimental measurements at different bridges were conducted with state-of-the-art IATSs and accelerometers as reference sensors.

1 INTRODUCTION

Conventional sensors for vibration-based SHM include accelerometers and robotic total stations. Both sensors comprise the disadvantage that access to the structure is required to attach the measurements sensor (accelerometer) or auxiliary equipment such as retroreflective prisms for total station measurements.

Therefore, the usage of an IATS for frequency measurements of oscillating structures has been proposed. Hereby, different prototypes with artificial (Bürki et al. 2010; Wagner et al. 2013; Charalampous et al. 2015) and natural targets (Wasmeier 2009; Hauth et al. 2013) were used. Furthermore, different state-of-the-art instruments were also tested with artificial (Ehrhart and Lienhart 2015a) and natural targets (Ehrhart and Lienhart 2015b; Ehrhart and Lienhart 2015c).

When using a single instrument, accurate measurements are only possible for movements parallel to the image sensor of the IATS. A two-instrument approach provides 3D measurements but requires a precise synchronization between the used IATSs and obviously a second instrument (Guillaume et al. 2016).

In this article, a single-instrument approach for accurate vibration measurements is proposed. Hereby, natural features of the observed structure are used as targets. By analyzing the

structure's directions of movement, it is not required to position the instrument so that the movements occur parallel to the image sensor of the IATS.

2 MEASUREMENT SYSTEM

The proposed sensor for measuring the frequencies of oscillating structures is an image-assisted total station (IATS, Figure 1). An IATS enhances a conventional robotic total station by an image sensor in the telescope in which the image data benefits from the optical magnification (e.g. 30x) of the telescope. Further descriptions of the multi-sensor system IATS can be found in Wagner et al. (2014). It is noted that recent generations of IATSs are available as scanning total stations which comprise a laser scanning functionality with measurement rates of up to 1 kHz (Leica 2015) or 26 kHz (Trimble 2016).

The image-based angle measurements H_z and V of an IATS comprise

- the values of the angle encoders,
- the readings of the two-axis tilt compensator, and
- the measured image coordinates of the target.

The computation of H_z and V and the necessary system calibration is compactly described by e.g. Bürki et al. (2010) or Ehrhart and Lienhart (2016). Ehrhart and Lienhart (2016) report an accuracy of 0.1 mgon (= 1.6 μ rad) for the image-based angle measurements of the instruments used in the case studies of this article. At a distance of e.g. 30 m between the IATS and the observed target, the reported accuracy corresponds to about 0.05 mm for the measured movements. The image coordinates of the natural features included in the observed structure (Figure 1) are obtained by feature matching which is robust for outdoor applications (Ehrhart and Lienhart 2015c).

The IATSs used in this article are a Leica MS50 I R2000 (Leica 2013), cf. Section 4.1, and a Leica MS60 I R2000 (Leica 2015), cf. Section 4.2. Concerning the image data, the instruments differ in the video rate and in the size of the video. Hereby, a 320 px \times 240 px video is transmitted at 10 fps for the MS50 and a 640 px \times 480 px video is transmitted at 30 fps for the MS60.

3 PROPOSED MEASUREMENT CONCEPT

For measurements with an IATS, the 3D Cartesian coordinates of a target \mathbf{x} are computed from the image-based angle measurements H_z and V and the slope distance s by

$$\mathbf{x} = s \begin{bmatrix} \cos H_z \sin V \\ \sin H_z \sin V \\ \cos V \end{bmatrix} = s \mathbf{v} \quad (1)$$

in which the origin of the coordinate system is set to the center of the IATS.

For a Leica MS60, the image-based angle measurements are available with an accuracy of 0.1 mgon and a measurements rate of 30 fps (Section 2). The accuracy of the reflectorless distance measurement is specified with 2 mm + 2 ppm in which a non-constant measurement rate of up to 20 Hz can be achieved (Leica 2015; Lienhart et al. 2017). Furthermore, for rapidly moving structures the distance measurements cannot be performed exactly towards the visual target because it is not possible to steer the telescope fast enough.



Figure 1. Exemplary setup for the monitoring of bridge vibrations with an IATS (bottom left) and observed image data with automatically detected features of the structure (bottom right).

However, if the observed element of the structure can be approximated by a triangulated irregular network (Gong et al. 1998) or a geometrical primitive (Scherer 2007), such as the plane in Figure 2, the distance can be computed. A plane can be described by the Hesse normal form

$$\mathbf{n} \cdot \mathbf{x} - d = 0 \quad (2)$$

where its parameters \mathbf{n} and d result from a plane fit of points on the structure's surface which are measured by the IATS. By inserting (1) in (2), the distance can be computed after

$$s = d (\mathbf{n} \cdot \mathbf{v})^{-1} \quad (3)$$

For applying (3), it is necessary that the surface points, from which the plane parameters are estimated, and the image-based angle measurements towards the visual target refer to the same coordinate system XYZ (Figure 2). Since both measurement types are obtained by using the same sensor, i.e., the IATS, this prerequisite is fulfilled.

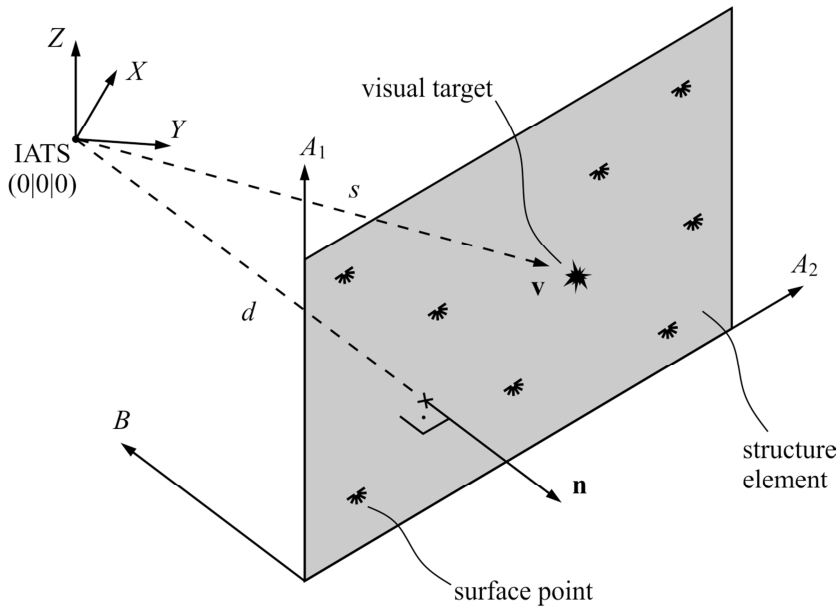


Figure 2. Element of an observed structure approximated by a plane.

It is however noted that the distance computed from (3) is only rigorously valid as long as the observed structure moves along the axes A_1 and A_2 . Movements along B can be detected by evaluating (1) in which the distance s is measured by a reflectorless distance measurement. It is hereby not necessary that the telescope points towards the visual target. The resulting coordinates \mathbf{x}^* can be used in

$$d^* = \mathbf{n} \cdot \mathbf{x}^* \quad (4)$$

to update the plane parameter d^* . The differences

$$b = d^* - d \quad (5)$$

correspond to the movements along B in Figure 2.

However, as already mentioned, the distance measurements are inferior to the image-based angle measurements. It is therefore beneficial if the movement axes of the observed structure are known prior to the selection of the instrument position. For monitoring applications according to DIN 18710-4, the expected movements of the observed structure are included in the task description.

Figure 3 depicts different instrument positions P , and thus different measurement geometries, for the monitoring of a bridge. The movement axes of the bridge are defined in vertical direction M_1 and across M_2 and along M_3 the bridge axis. Compared to M_1 and M_2 , it can be assumed that the movements along M_3 are much smaller.

For instrument position P_1 where the element E_1 is observed, the movements along B in Figure 2 correspond to the small movements along M_3 of the bridge in Figure 3. Consequently, the computation of the slope distance after (3) is valid and instrument position P_1 can be regarded as a favorable measurement geometry. For instrument position P_2 in the riverbed where the structure element E_2 is observed from a skew angle, (3) is not rigorously valid. Accordingly, instrument position P_2 can be regarded as an unfavorable measurement geometry.

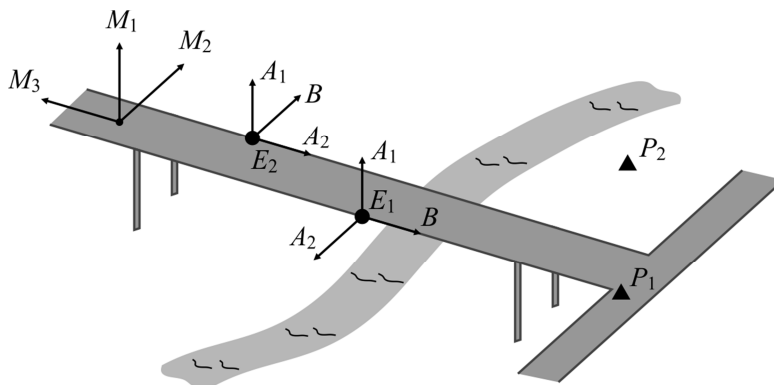


Figure 3. Monitoring of elements E of a bridge with movement axes M from different instrument positions P .

Summarizing, a favorable measurement geometry occurs if the movements of the structure along A_1 and A_2 (Figure 2) occur parallel to the image sensor of the IATS and the movements B are small.

4 CASE STUDIES

The suitability of different state-of-the-art IATSs for vibration-based SHM of oscillating structures was evaluated at the Augartensteg (steel construction, 74 m span width) and the Pongratz-Moore-Steg (steel construction, 72 m span) which are both footbridges over the river Mur in Graz, Austria.

For the Augarten measurements a Leica MS50 with a video rate of 10 fps (cf. Section 2) was used in which the instrument was positioned so that the favorable measurement geometry P_1 of Figure 3 is achieved. The Pongratz-Moore measurements were conducted by using a Leica MS60 with a video rate of 30 fps. Hereby, the instrument position P_2 of Figure 3 was chosen on purpose to evaluate the impact of an unfavorable measurement geometry. The accelerometers HBM B12/200 with a sampling rate of 200 Hz were used as reference sensors in both experiments. For both experiments, the distance between the IATS and the respective target was about 30 m.

4.1 Results for a favorable measurement geometry

For the Augarten experiment, Figure 4 shows the bridge response caused by one walker crossing the bridge. The instrument position P_1 (Figure 3) allows an accurate measurement of the movements in vertical direction and across the bridge axis. The movements along the bridge axis can only be determined from reflectorless distance measurements which are inferior to the accurate image-based angle measurements (cf. Section 3). Compared to the vertical movements with an amplitude of about 0.8 mm, the movements across the bridge axis with an amplitude of less than 0.3 mm are much smaller. However, the dominant frequency of 1.7 Hz, which also results from the accelerometer measurements, can be detected for both directions.

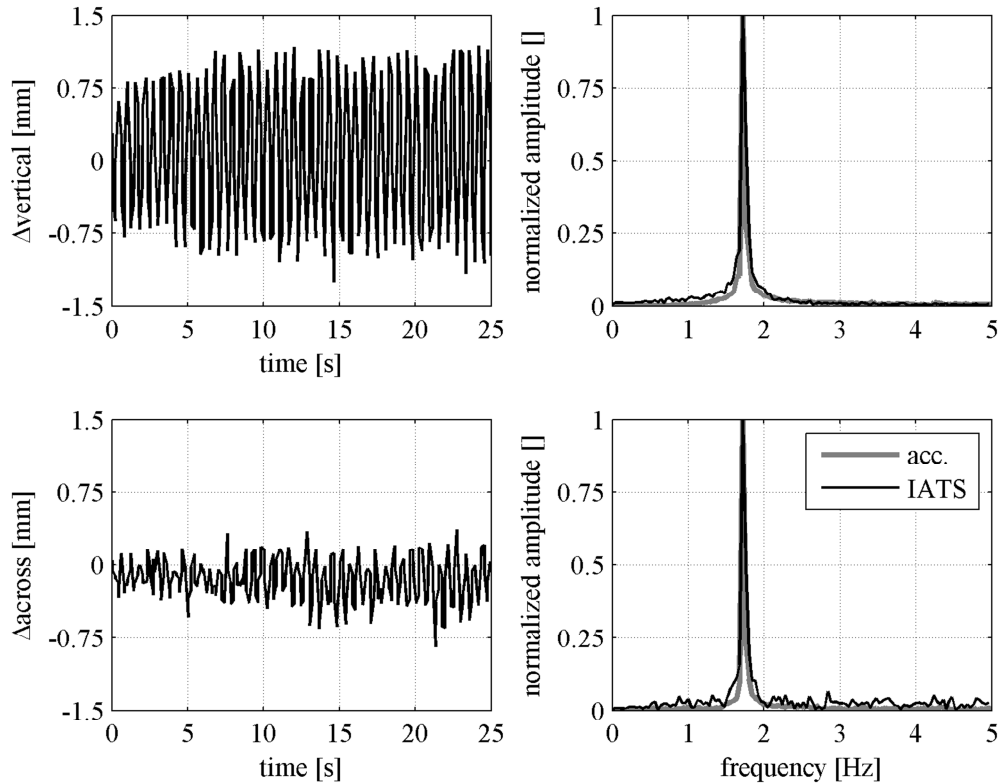


Figure 4. Bridge response in the Augarten experiment for one walker crossing the bridge.

4.2 Results for an unfavorable measurement geometry

For the Pongratz-Moore experiment, Figure 5 shows the vertical bridge response caused by two runners crossing the bridge. Although an unfavorable measurement geometry P_2 (Figure 3) was chosen for the measurements, the dominant frequency of 2.5 Hz, which corresponds to the step frequency of the runners, can be detected by using the approach of Section 3.

The movements along the bridge axis are too small to be resolved by the IATS. Furthermore, the dominant frequency of 32 Hz, measured by the accelerometer, could not be resolved by the IATS because of the video rate of 30 fps.

The movements across the bridge axis result from (5) and primarily depend on the reflectorless distance measurement of the IATS. Due to the limited accuracy of the distance measurements (Section 3), the resulting amplitude spectrum does not contain reasonable information.

However, Figure 6 depicts the time series of the movements across the bridge axis, resulting from (5), for the duration of the experiment. Additionally, measurements with a robotic total station (RTS), which were taken at instrument position P_1 (Figure 3) and thus allow an accurate measurement of the across movements, are displayed. Both time series are filtered by a low-pass Butterworth filter of order 2 and a cutoff frequency of 0.5 Hz.

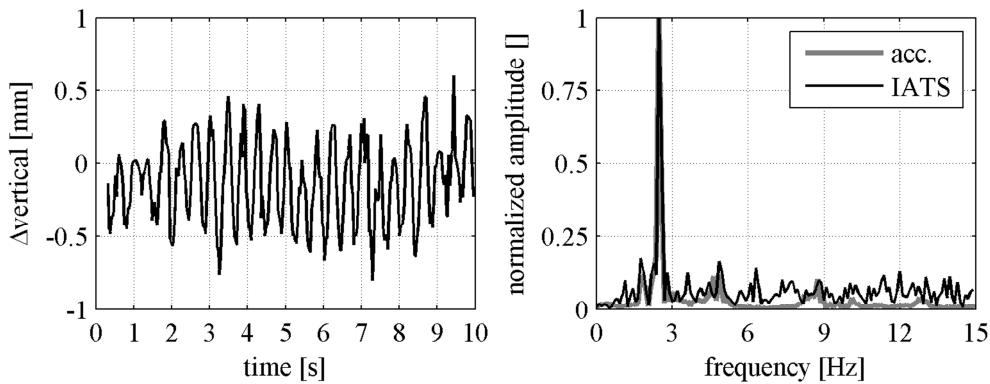


Figure 5. Vertical bridge response in the Pongratz-Moore experiment for two runners crossing the bridge.

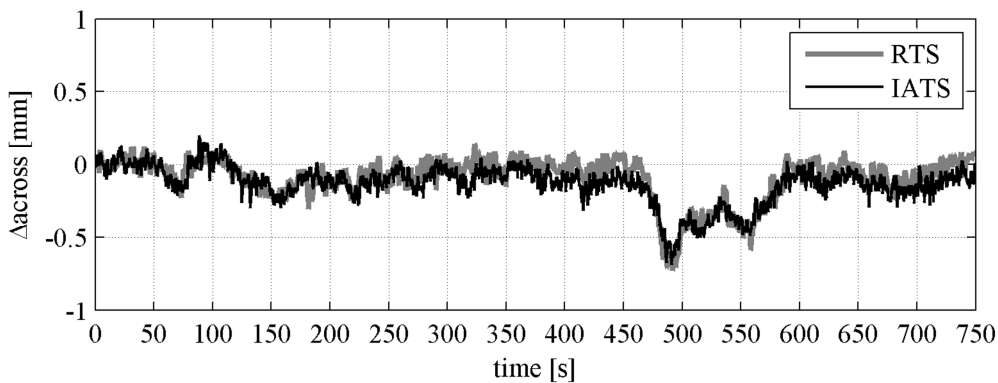


Figure 6. Filtered bridge response across the bridge axis in the Pongratz-Moore experiment.

The correspondence between the two time series validates the approach of Section 3. It is noted that the events in the times series can be related to wind loads acting on the bridge. Figure 6 also demonstrates that the specified accuracy of the reflectorless distance measurement of 2 mm + 2 ppm (Section 3) is outperformed for relative distance measurements.

5 CONCLUSIONS

In this article it was shown that state-of-the-art IATSs can be used for vibration-based SHM, i.e., for frequency measurements of oscillating structures. By analyzing the structure's directions of movement, the measurement geometry can be designed so that the relevant movements occur parallel to the image sensor of the IATS which allows accurate measurements with measurement rates of (currently) 30 Hz.

Compared to conventional measurements with robotic total stations or accelerometers, an IATS has the advantage that access to the observed structure is not required at any time. This is achieved by observing natural features of the structure with the IATS's telescope camera. Compared to accelerometer measurements, an IATS is further advantageous because it allows the analysis of the oscillations also in time domain.

It was shown that the specified accuracy of a few millimeters for the reflectorless distance measurement of recent IATs can be outperformed for relative measurements occurring in monitoring applications. The relatively low measurement rate of the distance measurements (less than 20 Hz) could be improved by using the hardware of recent scanning total stations which allows measurement rates in the kHz range.

6 REFERENCES

- Bürki, B., S. Guillaume, P. Sorber, and H. Oesch, 2010, DAEDALUS: A Versatile Usable Digital Clip-on Measuring System for Total Stations. *Proc. 2010 International Conference on Indoor Positioning and Indoor Navigation (IPIN)*, 1-10.
- Charalampous, E., P. Psimoulis, S. Guillaume, M. Spiridonakos, R. Klis, B. Bürki, M. Rothacher, E. Chatzi, R. Luchsinger, and G. Feltrin, 2015, Measuring sub-mm structural displacements using QDaedalus: a digital clip-on measuring system developed for total stations. *Applied Geomatics*, 7(2): 91-101.
- DIN 18710-4 2010-09. Ingenieurvermessung - Teil 4: Überwachung.
- Ehrhart, M., and W. Lienhart, 2015a, Image-based dynamic deformation monitoring of civil engineering structures from long ranges. *Proc. SPIE 9405, Image Processing: Machine Vision Applications VIII*, 94050J.
- Ehrhart, M., and W. Lienhart, 2015b, Development and evaluation of a long range image-based monitoring system for civil engineering structures. *Proc. SPIE 9437, Structural Health Monitoring and Inspection of Advanced Materials, Aerospace, and Civil Infrastructure 2015*, 94370K.
- Ehrhart, M., and W. Lienhart, 2015c, Monitoring of Civil Engineering Structures using a State-of-the-art Image Assisted Total Station. *Journal of Applied Geodesy*, 9(3): 174-182.
- Ehrhart, M., and W. Lienhart, 2016, Accurate Measurements with Image-Assisted Total Stations and Their Prerequisites. *Journal of Surveying Engineering*, Online publication date: August 3, 2016.
- Gong, D., Y.D. Huang, and S.L. Ball, 1998, A laser scanning videotheodolite for 3D visualisation and metrology. *ISPRS Archives XXXII-5*, 1-5.
- Guillaume, S., J. Clerc, C. Leyder, J. Ray, and M. Kistler, 2016, Contribution of the Image-Assisted Theodolite System QDaedalus to Geodetic Static and Dynamic Deformation Monitoring. *Proc. 3rd Joint International Symposium on Deformation Monitoring (JISDM)*, 1-9.
- Hauth, S., M. Schlüter, and F. Thiery, 2013, Schneller und ausdauernder als das menschliche Auge: Modulare Okularkameras am Motortachymeter. *Allgemeine Vermessungs-Nachrichten*, 120(6): 210-216.
- Leica, 2013, Leica MS50/TS50/TM50 User Manual. Leica Geosystems AG, Heerbrugg, Switzerland. 84p.
- Leica, 2015, Leica MS60/TS60 User Manual. Leica Geosystems AG, Heerbrugg, Switzerland. 90p.
- Lienhart, W., M. Ehrhart, and M. Grick, 2017, High frequent total station measurements for the monitoring of bridge vibrations. *Journal of Applied Geodesy*, 11(1): 1-8.
- Scherer, M., 2007, Phototachymetrie: Eine Methode zur Bauaufnahme und zur Erstellung eines virtuellen Modells. *Allgemeine Vermessungs-Nachrichten*, 114(8-9): 307-313.
- Trimble, 2016, Trimble SX10 Scanning Total Station Datasheet. Trimble Navigation Limited, Sunnyvale, California. 4p.
- Wagner, A., P. Wasmeier, C. Reith, and T. Wunderlich, 2013, Bridge Monitoring by Means of Video-Tacheometer - A Case Study. *Allgemeine Vermessungs-Nachrichten*, 120(8-9): 283-292.
- Wagner, A., P. Wasmeier, T. Wunderlich, and H. Ingensand, 2014, Vom selbstzielenden Theodolit zur Image Assisted Total Station. *Allgemeine Vermessungs-Nachrichten*, 121(5): 171-180.
- Wasmeier, P., 2009, Grundlagen der Deformationsbestimmung mit Messdaten bildgebender Tachymeter. Ph.D. thesis, DGK C-638, Technische Universität München, Munich, Germany.